

PACS numbers: 42.55. Lt; 42.60.Lh
DOI: 10.1070/QE2004v034n03ABEH002629

Pulse generator for pumping electric-discharge excimer lasers

I.N. Konovalov, Yu.N. Panchenko, M.Yu. Sukhov

Abstract. **A pulse generator is developed for pumping electric-discharge excimer lasers in which the capacitive energy storage is connected with the gas-discharge chamber of the laser with the help of a multichannel spark switch via a low-inductive strip line. This scheme of the generator reduces energy losses in the switch and the inductance of the discharge circuit of the capacitive storage. For the pump power equal to 800 MW, the efficiency of the stored energy transfer to a load achieves 85 %. To ignite a homogeneous volume discharge, the generator produces a prepulse, which initiates a low-current volume discharge in the gas-discharge chamber. Upon excitation of an electric-discharge XeCl laser with the $3 \times 5.4 \times 80$-cm active region and the $Ne : Xe : HCl = 2000 : 2.5 : 1$ mixture at a pressure of 4 atm, radiation pulses with energies up to 3.4 J and the FWHM duration up to 260 ns were obtained with a homogeneous energy distribution over the laser aperture.**

Keywords*: pulse generator, volume discharge, XeCl laser.*

1. Introduction

Great progress in the development of electric-discharge lasers with pulse energies from 1 to 10 J was achieved by using capacitve storage lines with the wave resistance of no more than 1 Ω in pump generators [1 – 8]. To ignite a self-sustained volume discharge, a high-voltage is used, which is formed by a peaking capacitor of the discharge circuit of the pump generator or is fed to the lead of the gas-discharge camera from an additional charging capacitor. The reduction of the formation time of the volume discharge due to a rapid rise of the voltage across the interelectrode gap of the gas-discharge chamber and charging of the water-cooled storage line to the doubled voltage of the quasi-stationary discharge burning provided the efficiency of energy transfer from the line to the active laser medium amounting to 93 % [1]. The improvement of the homogeneity of the volume discharge and the optimisation of the electric-field strength in the plasma provided the pump efficiency for a XeCl laser amounting up to 5 % [5]. As mentioned before [1, 7, 8], a further increase in the efficiency of electric-discharge excimer lasers can be achieved by improving the volume discharge homogeneity, increasing the current rise rate in the discharge and decreasing energy losses in a switch.

To reduce the switching time and, hence, energy losses in the switch in the case of a series connection of the capacitive energy storage, switch, and load, a lumped or distributed 'heating' capacitance was connected in parallel with the switch [9, 10]. Such a connection of the switch results in high total inductance of the discharge circuit so that its dimensions should be as small as possible. By contrast, the switch in the pulse generator based on a double capacitive line is taken out of the line discharge circuit and is connected with the load, so that no restrictions are imposed on its dimensions. The charging voltage of this generator is less by half than the voltage used in a generator with one capacitive storage. However, during the voltage inversion in one of the capacitive lines of the generator, the switching current is greater by a factor of two than in the generator with one line. This results in high energy losses in the switch and in the elongation of the leading edge of the voltage pulse across the load.

To increase the efficiency of utilisation of the energy stored in the generator by decreasing energy losses in the switch and reducing the inductance of the discharge circuit of the generator, we developed a pulse generator for pumping electric-discharge excimer lasers, in which the capacitive energy storage is connected to the gas-discharge chamber of the laser with the help of a multichannel spark switch via a low-inductive strip line. To ignite a homogeneous volume discharge, the generator forms a prepulse, which produces a low-current volume discharge in the gas-discharge chamber of the laser.

2. Experimental setup

Figure 1 shows the principal electric scheme of the generator. The energy storage C_L consists of two parallel-connected lines with a film insulation (FL-100 or FL-200 films) or with a film – paper – oil insulation (FL-300), which were developed at the Novik Development Bureau and had the 'electric length' 100, 200, and 300 ns, the capacitance 50, 100, and 150 nF, respectively, and the wave resistance 1 Ω. The lines were charged by pulses from a IK 100-kV, 0.4-μF capacitor C_{ac} via a KVI-120 cable upon commutation of coaxial controlled spar gap (*1*) [11]. The charging inductance $L_2 = 1$ μH and resistance $R_4 = 2.4$ Ω were made in the form of a coil of a Nichrome wire 0.5 mm in diameter. The voltage pulses across the capacitive lines and the lead

I.N. Konovalov, Yu.N. Panchenko, M.Yu. Sukhov Institute of High-Current Electronics, Siberian Branch, Russian Academy of Sciences, prosp. Akademicheskii 4, 634055 Tomsk, Russia;
e-mail: losev@ogl.hcei.tsc.ru

Received 3 July 2003
Kvantovaya Elektronika **34** (3) 289 – 293 (2004)
Translated by M.N. Sapozhnikov

of gas-discharge chamber (*3*) were detected using voltage dividers R_2, R_3 and R_5, R_6. The discharge current of the storage lines was measured with the help of shunts R_1. The shunts were made of 0.5-W, 1-Ω TBO composition resistors, which were uniformly distributed over the width of the lines.

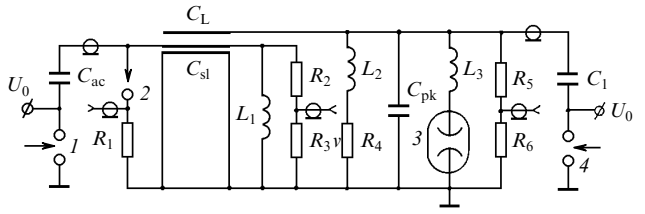

Figure 1. Electric scheme of the generator: (*1*, *4*) spark gaps; (*2*) switch; (*3*) gas-discharge chamber; (C_L) energy storage; (C_{sl}) strip line inductance; (C_{pk}) peaking capacitor; (C_{ac}) storage capacitor; (U_0) charging voltage.

A two-electrode multichannel spark gap with a strongly inhomogeneous electric field near the anode was used as fast low-inductive switch (*2*). The electrodes of the spark gap were made of stainless steel. The anode was a plate of thickness 1 mm and the cathode was a rod of diameter 15 mm. The length of the electrodes was 680 mm and the gap between them was 6 mm. To provide the stable triggering and multichannel breakdown of the spark gap, it was illuminated by sparks ignited near the cathode during triggering. The gap housing was made of a polyvinyl chloride plastic tube with the external diameter of 65 mm. During charging storage lines up to 40–60 kV, the multichannel gap was filled with nitrogen up to pressures of 1.5–2.5 atm. A similar spark gap with a metal housing and water-cooled electrodes for a repetitively pulsed pump generator was developed in Ref. [11].

The strip line had the capacity $C_{sl} = 5$ nF, the 'electric length' $t_{sl} = 10$ ns, and the wave resistance $\rho_{sl} = 1$ Ω and was formed by the lower buses of storage lines and a grounded current-carrying bus of the generator, which were separated by a polyvinyl chloride plastic or polyethylene sheet. The pump generator used a two-circuit scheme with the peaking capacitor $C_{pk} = 4.9$ nF, which was responsible for the formation of a volume discharge in the gas-discharge chamber. The peaking capacitor was assembled of KVI-3 ceramic capacitors (20 kV, 680 pF). The breakdown of the multichannel spark gap occurred under the action of the capacitor $C_1 = 6.6$ nF charged up to 60 kV. The discharge current of the capacitor C_1 was switched with controlled spark gap (*4*).

The electric parameters and dimensions of the strip line of the pump generator can be determined from the following conditions. For the given size of the active region of the laser, the composition and pressure of the working gas mixture, the pump regime of the laser is determined by the charging voltage U_0 across the storage lines of the pulse generator and by the amplitude I_c of the volume discharge current. The wave resistance of the strip line should satisfy the condition $\rho_{sl} = U_0/I_c$, the 'electric length' t_{sl} of the line should be equal to the time t_c required for achieving the discharge current I_c in switch (*2*) [11]. The capacitance of the strip line can be determined from the relation $\rho_{sl} = t_{sl}/(2C_{sl})$ and the known expression $C_{sl} = \varepsilon_0 \varepsilon S/a$, where $S = lb$ is the area of the smaller of the current-carrying plates forming the line. This gives the dimensions of the strip line,

$$\frac{a}{b} = \frac{U_0}{I_c} c\varepsilon_0 \sqrt{\varepsilon}, \tag{1}$$

$$l = \frac{t_c c}{2\sqrt{\varepsilon}}, \tag{2}$$

where a is the thickness of the strip line dielectric (in m); b is the strip line width (in m); c is the speed of light (in m s^{-1}); ε_0 is the dielectric constant (in F m^{-1}); and ε is the relative dielectric constant.

A rapid rise of the voltage across the strip line during charging from the capacitor C_1 and an increase in the electric field strength near the anode in the spark gap produce multichannel current switching when the gap breakdown voltage is achieved. When the number of spark channels is large and the average current in the channel is less than 10 kA, the time constant τ_R of the exponential decay of the voltage across N parallel channels during the first ~ 50 ns after the gap breakdown onset can be determined by using the combined empirical Martin formula [12]

$$\tau_R = \frac{L}{NR} + 88 d^{1/3} R^{-1/3} E_0^{-4/3} \delta^{1/2} N^{-1/3}, \tag{3}$$

where d is the distance between the anode and cathode in the gap (in cm); R is the generator impedance (in Ω); E_0 is the initial electric field strength along the channel (in units of 10 kV cm^{-1}); δ is the ratio of the air density in the interelectrode gap to its density at normal temperature and pressure; $L \approx 14d$ is the channel inductance (measured in nH).

During the discharge of the strip line and then of the storage lines of the pump generator, the rise in the current in the spark channels of the gap mainly depends on the velocity of gas-dynamic expansion of the channels, which is $\sim 10^6$ cm s^{-1} [13, 14]. The temperature of the nitrogen plasma in channels achieves $(2-3) \times 10^4$ K and the electron density is $\sim 2 \times 10^{17}$ cm^{-3}. Due to conversion of singly charged nitrogen ions, the concentration of N_2^+ ions increases up to 10^{17} cm^{-3}. Under these conditions, the characteristic time of dissociative recombination of electrons and molecular nitrogen ions is shorter than 1 ns. To maintain the increasing conductivity of the plasma in all the spark gaps formed, the rate of the current rise in the discharge circuit of the generator should be close to 10^{12} A s^{-1} during the gap switching time t_c. When the rate of the switched current rise is limited and achieves its maximum value, the current is redistributed between channels formed earlier and channels formed later.

Due to the presence of inductance of the line between spark gaps, this can produce a substantially inhomogeneous voltage distribution between the channels and a more considerable difference between currents in the channels [9]. As a result, the active resistance of the gap and losses in it will increase, and the front of the voltage wave incident on the peaking capacitor of the generator and the lead of the gas-discharge chamber will be distorted. In this connection, provision should be made for providing the multichannel breakdown of the gap with a small time scatter [15]. The inductance of the connection of the strip line with the gap and the load inductance should be as small as possible.

The own parameters of storage lines of the generator are very important because they determine the amplitude and the maximum rate of the discharge current rise. For the line with distributed parameters, we have

$$\rho_{C_L} = \frac{377a}{b\sqrt{\varepsilon}}, \tag{4}$$

$$\frac{I_a}{b} = 2.65 \times 10^{-3} E\sqrt{\varepsilon}, \tag{5}$$

where I_a is the current amplitude in the short-circuited line; E is the electric field strength in insulation; and ρ_{C_L} is the wave resistance of the line. It follows from (4) and (5) that the maximal possible current from the line is determined by the dielectric constant of the insulation, its electric strength, and the line dimension. To obtain large current, it is necessary to use dielectrics with a great value of $E\sqrt{\varepsilon}$. For pulse generators with low-resistance lines, water is in fact the most convenient dielectric. However, a line with water insulation has rather large dimensions, and the additional equipment is required to purify water from impurities.

The generator developed by us uses lines with the film or film – paper – oil insulation because they are compact and are simple in service. In particular, FL-200 lines have the width 285 mm, height 90 mm, and length 270 mm, and are designed to operate at the charge-discharge repetition rate up to 100 Hz at the nominal charging voltage equal to 70 kV. The FL-200 lines were successfully used for pumping a wide-aperture electric-discharge laser. The output pulse energy of 14 J was obtained at the efficiency of the energy storage in lines equal to 4 % [6].

Our study of a wide-aperture electric-discharge XeCl laser showed [16, 17] that preionisation of the Ne – Xe – HCl working gas mixture up to the initial electron concentration $n_0 \geqslant 10^{12}$ cm^{-3} improved the homogeneity and stability of a self-sustained volume discharge. In this connection, we provided the formation of a prepulse in our generator, which produced a low-current volume discharge in the gas-discharge chamber to ignite a homogeneous volume discharge. Upon charging storage lines C_L from the capacitor C_{st} for 2.5 μs, the voltage up to 10 kV appears across the resistance R_4, which is applied to the peaking capacitor C_{pk} and the discharge gap of gas-discharge chamber (*3*) (Fig. 1).

After preionisation of the working gas mixture with an X-ray source, a homogeneous luminous volume discharge with the electron concentration of the order of 10^{12} cm^{-3} is ignited in the discharge gap [18]. When the breakdown of a multichannel spark gap is initiated by a voltage pulse from the capacitor C_1, it is desirable to select parameters of the discharge gaps of the gas-discharge chamber and multichannel spark gap so that, for the specified steepness of the voltage rise on them, the breakdown voltage of the spark gap would be close to the maximum voltage achieved during the volume discharge formation. In this case, burning of the low-current volume discharge in the active region of the laser is enhanced for a short time.

3. Experimental results

The experimental study of regimes of the discharge of the FL-100 and FL-200 lines in our pulse generator on the 0.5-Ω low-inductive active load matched with the lines showed that the scheme of the generator compares well with the capacitive line – switch – load scheme even at the minimum size of the switch built in the load. During the discharge of storage lines, the strip line operates as a low-inductive element of the discharge circuit.

The voltage drop across the gap and the discharge current of the lines were measured simultaneously at several points along the gap length. The results of these measurements and the observation of emission of spark channels through windows at the ends of the gap housing made it possible to estimate the development dynamics of spark channels and the distributions of the channels and switched current along the gap length. As the charging voltage across the storage lines was increased from 40 to 60 kV, the breakdown of the gap occurred along many spark channels (30 – 40 over 1 m of the gap length). In addition, 6 – 8 diffusion channels, probably related to the scattering of energy at the pump pulse end, were observed against the background of spark channels. In this case, the scatter in the measurements of the switched current decreased from 30 % to ~ 10 %. For the charging voltages across storage lines less than 40 kV, the multichannel current switching was achieved without changing the configuration of the gap electrodes by filling the gap with helium up to pressures of 3 – 5 atm. The operation of the multichannel gap was most stable when the pump generator was discharged on the short-circuited load or the load of a few fractions of ohm because the rise rate and amplitude of the discharge current were the largest for the specified charging voltages across storage lines.

The total discharge current of storage lines was calculated taking into account the inhomogeneity of its distribution over the length of electrodes of the multichannel gap. The results of calculations were verified by comparing the charge passed over the circuit and the observed change in the voltage across storage lines, as well as by measuring the voltage drop across the active load of the generator. The energy losses in the multichannel gap were estimated from the oscillograms of the voltage decrease across the gap and of the current rise in the circuit taking into account the voltage drop across the gap inductance.

The dynamics of variation in the active resistance of the multichannel gap during the discharge of the FL-200 storage line on a matched load is shown in Fig. 2a. After spark-gap breakdown, the rate of the voltage decrease across the gap achieves 5×10^{12} V s^{-1} during the first ~ 10 ns. However, during the following 50 ns this rate decreases down to 2×10^{11} V s^{-1} and then becomes equal to 2×10^{10} V s^{-1} on average. As a result, during the rise time of the current in the circuit, the voltage across the interelectrode gap is between 5 and 3 kV, while the active resistance of spark channels changes from 1 to 0.3 Ω. When the discharge current amplitude corresponding to the maximum pump pulse power is achieved, the active resistance of spark channels is ~ 10 % – 20 % of the load resistance. As the current amplitude in the circuit increases from 20 to 80 kA, the gap resistance decreases exponentially from 0.15 down to 0.035 Ω.

When the FL-100 or FL-200 storage lines were used in the generator in which a Dacron insulation film was wetted with transformer oil or carbogal (dimethyl cyclohexane), respectively, without the use of a capacitor paper, the generator could produce pump pulses of power up to 800 MW, with the 85 % efficiency of energy transfer to the load. As the discharge power further increased, the

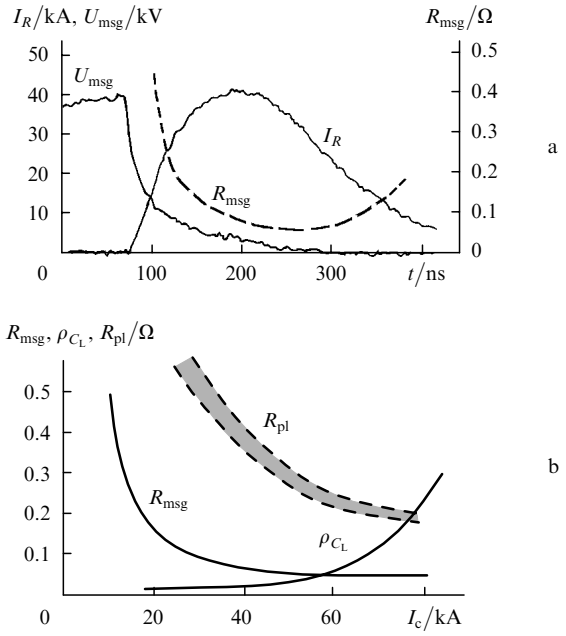

Figure 2. Dynamics of variations in the voltage U_{msg} across the multichannel gap and the active resistance R_{msg} during the discharge of the generator with current I_R to the matched load (a) and the dependences of the active resistance R_{msg}, the resistance ρ_{C_L} of active losses in storage lines and the resistance R_{pl} of the volume discharge plasma on the current I_c of the generator discharge (b) for the $3 \times 5.4 \times 80$-cm active region of the laser, the mixture composition Ne : Xe : HCl = (1500 – 2000) : (2 – 5) : 1, and a pressure of 4 atm.

dielectric losses drastically increased in the lines and the fraction of energy supplied to the load decreased. When the lines were discharged in the short-circuited regime, the rate of the current rise in the circuit did not exceed 6×10^{11} A s^{-1}, and the current amplitudes were ~ 0.75 of the amplitudes calculated by dividing the charging voltage by the wave resistance of the lines. In the FL-300 lines, the combined film – paper – oil insulation was used. For output powers exceeding 600 MW, the active losses in the lines achieved 50 % of the stored energy. When the FL-300 lines were short-circuited, the rate of the discharge current rise did not exceed 2×10^{11} A s^{-1}, while the current amplitude was ~ 0.5 of the calculated value.

Figure 2b shows the dependences of the active resistance of the multichannel spark gap and the active resistance of the FL-200 storage lines on the discharge current of the generator on the load (a successive scheme of the replacement of a dielectric with losses was used in calculations). A comparison of these dependences with the resistance of the volume-discharge plasma in an electric-discharge XeCl laser, which we studied earlier [6, 16, 17], shows that, when the discharge current in the generator is below 30 kA and, hence, the specific pump power of the laser is comparatively low (less than 300 kW cm^{-3}), the energy losses in the generator and the macroscopic inhomogeneity of the pump of the active medium of the laser will be mainly determined by the multichannel gap. Therefore, the configuration of the interelectrode gap and its switching parameters should be properly selected for the given discharge regime of the generator.

For the discharge current 30 – 60 kA, when the specific pump power increases from 300 to 500 kW cm^{-3}, the pump regimes are optimal in the efficiency of stored energy transfer to the volume-discharge plasma (up to 85 %) and in the efficiency of energy conversion to light (up to 4.7 %) [6]. Charging storage lines in the generator up to voltages above 60 kV and the achievement of the discharge-current amplitude above 60 kA will result in a further linear increase in the pump power of the laser and the output pulse energy [16]. However, because of the increase in dielectric losses in the lines, the lasing efficiency will decrease drastically.

We used the developed generator to pump the electric-discharge XeCl laser with the active region of size 3 cm × 5.4 cm × 80 cm. The inductance of the discharge chamber was $L_3 \sim 20$ nH. The aim was to obtain radiation pulses of energy up to 2 J and the FWHM duration of no less than 250 ns. For this purpose, we employed the FL-300 lines with the 300-ns 'electric length' in the pump generator. The working gas mixture in the gas-discharge chamber had the composition Ne : Xe : HCl = 2000 : 2.5 : 1 at a pressure of 4 atm. The gas mixture was preionised by 25 – 30-kV, 500-ns soft X-ray pulses. The radiation source provided homogeneous ionisation of the gas in the active region of the laser and produced the initial electron concentration up to 2×10^9 cm^{-3} in the absence of voltage across the discharge gap [16, 19]. The optical resonator consisted of a dielectric mirror with the 99 % reflectivity at a wavelength of ~ 308 nm and a plane – parallel quartz plate. The laser pulses were detected with a FEK-22 photodiode and the output energy was measured with an IMO-2H calorimeter.

Figure 3 shows the oscillograms of voltage, current, and emission pulses, which characterise the operation of the pump generator, the supply of energy to the active medium of the laser, and lasing. After breakdown of the multichannel gap at the maximum of the charging voltage pulse across capacitive storage lines, the strip line is discharge to the gap and the voltage from the storage lines is supplied to recharge a peaking capacitor. In this case, the steepness of the voltage rise and the voltage amplitude on the peaking capacitor are no less than for a conventional two-circuit scheme of the pump generator.

During the formation of a self-sustained volume discharge and the rise of a discharge current in the active region of the laser, the oscillating discharge of the peaking capacitor via the multichannel gap maintains the conductivity of spark channels in the gap and their homogeneous distribution over the gap length. The best operating regimes of the laser were obtained when the formation of the volume discharge was delayed by 350 – 400 ns with respect to the X-ray pulse onset. By this time, X-ray radiation, maintaining a low-current volume discharge, achieved the maximum intensity and the rate of formation of free electrons in the working gas mixture induced by X-rays was $\sim 10^{16}$ cm^{-3} s^{-1}. By charging the storage lines of the pump generator up to 45 kV, we obtained the 2.1-J, 260-ns output pulses with the homogeneous energy distribution over the 3×5.4-cm laser aperture. When the charging voltage in the lines was increased up to 60 kV, the output pulse energy was 3.4 J and the FWHM duration was 240 ns.

4. Conclusions

We have developed a pulse generator for pumping electric-discharge excimer lasers. The capacitive storage lines in the generator are connected to the load with the help of a

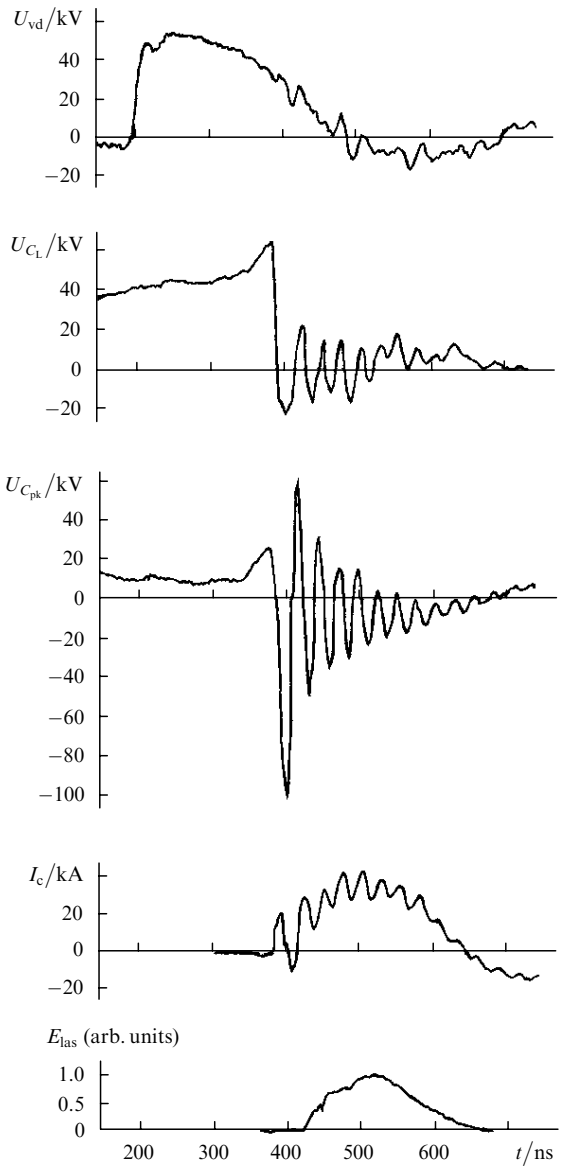

Figure 3. Oscillograms of voltage pulses on storage lines (U_{C_L}), peaking capacitor ($U_{C_{pk}}$), vacuum diode of the X-ray source (U_{vd}), the volume-discharge current I_c, and output emission E_{las} for the Ne : Xe : HCl = 2000 : 2.5 : 1 mixture at a pressure of 4 atm.

multichannel spark gap via a low-inductive strip line. The electric scheme of the generator provides the fast current switching in the discharge circuit and, resulting in low energy losses in the gap. In addition, the scheme improves the matching between the impedances of the storage lines of the generator and the load due to the reduction of the inductance between them.

Generators based on compact storage lines with the film insulation are capable of producing pump powers up to 800 MW, with the efficiency of energy transfer to the volume discharge achieving 85 %. The homogeneous and stable volume discharge was formed after the preliminary ignition of a low-current volume discharge with the electron concentration in the plasma of the active region of the laser equal to $\sim 10^{12}$ cm^{-3}. Upon excitation of pulses from the electric-discharge XeCl laser with the active region of size 3 cm × 5.4 cm × 80 cm by the generator, the homogeneous burning of the volume discharge of duration 500 ns was achieved at the specific pump power of 200–400 kW cm^{-3}, and 3.4-J laser pulses with the FWHM duration up to 260 ns and the homogeneous energy distribution over the laser aperture were produced.

References

1. Long W.H. Jr., Plummer M.J., Stappaerts E.A. *Appl. Phys. Lett.*, **43**, 735 (1983).
2. Fisher C.H., Kushner M.J., De Hart T.E., Mc Daniel J.P., Petr R.A., Ewing J.J. *Appl. Phys. Lett.*, **48**, 1574 (1986).
3. Taylor R.S., Leopold K.E. *Appl. Phys. B*, **59**, 479 (1994).
4. Van Goor F.A., Witteman W.J., et al. *Proc. SPIE Int. Soc. Opt. Eng.*, **2206**, 30 (1994).
5. Gerritsen J.W., Keet A.L., Ernst G.J., Witteman W.J. *J. Appl. Phys.*, **67**, 3517 (1990).
6. Basov V.A., Konovalov I.N. *Kvantovaya Elektron.*, **23**, 787 (1996) [*Quantum Electron.*, **26**, 767 (1996)].
7. Levatter J.I., Robertson K.L., Shao Chi Lin. *J. Appl. Phys.*, **39**, 297 (1981).
8. Van Goor F.A., Trentelman M., Timmermans J.C.M., Witteman W.J. *J. Appl. Phys.*, **75**, 621 (1994).
9. Koval'chuk B.M., Kremnev V.V., Potalitsyn Yu.F. *Sil'notocnye nanosekundnye kommutatory* (High-Current Nanosecond Switches) (Novosibirsk: Nauka, 1979).
10. Mesyatz G.A. (Ed.) *Moshchnye nanosekundnye impul'snye istocniki uskorennykh elektronov* (High-Power Nanosecond Pulsed Sources of Accelerated Electrons) (Novosibirsk: Nauka, 1974).
11. Balbonenko E.F., Basov V.A., Vizir' V.A., Konovalov I.N., Sak K.D., Chervyakov V.V. *Prib. Tekh. Eksper.*, (6), 86 (1997).
12. Martin J.C. *Multichannel Gaps* (Aldermaston, Berks: SSWA (JSM), 1970).
13. Drabkina S.I. *Zh. Eksp. Teor. Fiz.*, **21**, 473 (1957).
14. Braginskii S.I. *Zh. Eksp. Teor. Fiz.*, **34**, 1548 (1958).
15. Taylor R.S., Leopold K.E. *Rev. Sci. Instr.*, **55**, 52 (1984).
16. Balbonenko E.F., Basov V.A., Konovalov I.N., Sak K.D., Chervyakov V.V. *Prib. Tekh. Eksper.*, (4), 112 (1994).
17. Konovalov I.N. *Izv. Vyssh. Uchebn. Zaved., Ser. Fiz.*, **43**, 54 (2000).
18. Konovalov I.N., Koval' N.N., Suslov A.I. *Kvantovaya Elektron.*, **32**, 663 (2002) [*Quantum Electron.*, **32**, 663 (2002)].
19. Bychkov Yu., Kostyrya I., Makarov M., Suslov A., Yastremsky A. *Rev. Sci. Instr.*, **65**, 793 (1994).